Geophys. J. Int. (2000) **141,** 25–42

Autoregressive estimation of the splitting matrix of free-oscillation multiplets

Guy Masters, Gabi Laske and Freeman Gilbert
IGPP, Scripps Institution of Oceanography, La Jolla, CA 92093-0225, *USA. E-mail: glaske@ucsd.edu*

Accepted 1999 September 30. Received 1999 September 27; in original form 1999 March 26

SUMMARY

Recent, large earthquakes, recorded by the rapidly growing global seismic networks, have produced a vast amount of high-quality data. These new data allow us to develop new techniques to determine the coupling and splitting characteristics of multiplets, and hence determine the 3-D structure of the Earth. Current techniques tend to be computationally intensive and non-linear and require detailed models of earthquake sources (which might be unavailable for the large and often complicated events used in free-oscillation research). Here, we introduce a new technique that allows us to solve for the most general form of the splitting matrix in a few steps without knowledge of the earthquake sources.

The method takes advantage of the fact that certain linear combinations of seismograms for a single earthquake have an autoregressive property for which the propagator matrix is related to the exponentiated splitting matrix. To retrieve the propagator matrix, it is necessary to use only displacement scalars from a reference earth model and instrument calibrations to perform a two-step linear inversion. Multiple events can (and, generally, must) be used to allow retrieval of the propagator matrix. It is straightforward to recover the splitting matrix from the propagator matrix and it is the elements of the splitting matrix that provide linear constraints on the 3-D structure of the earth.

We illustrate the technique by using nearly 900 vertical-component recordings from 10 large earthquakes to recover the splitting matrices of a variety of multiplets. The results are presented as splitting functions, including some of the first robust anelastic splitting functions to be determined.

Key words: free oscillations, mode coupling, mode splitting.

INTRODUCTION

During the decade 1984–1993, when the Global Seismic Network was in its initial growth phase, progress in observational low-frequency seismology was modest. A lack of very large events and, in particular, a lack of very large *deep* events made progress difficult and incremental. The Fiji event in March 1994 did rekindle some interest (since it was the largest deep event to be digitally recorded since the 1970 Colombian event) but it was rapidly eclipsed by the Bolivian event in June 1994. Not only was the Bolivian event larger than the 1970 Colombian event but it was recorded by an unprecedented number of observatory-quality digital stations. The top two panels of Fig. 1 show details of a typical spectrum of a vertical-component recording of the event, illustrating the rich spectrum of high-Q overtones, which are sensitive to core structure. The anomalous splitting of multiplets such as ${}_{13}S_2$ is clearly visible. The event also excited other classes of modes that are sensitive to mantle structure and gave some very clear observations of low-order toroidal modes. Furthermore, on 1994 October 4, another great earthquake occurred but this time in the southern Kuril Islands. This event was roughly the same size as the Bolivian event and was at about 50 km depth. It also strongly excited overtones (bottom two panels of Fig. 1). Since then, several other large events have also produced usable recordings of overtones (Table 1) and we now have a significant new data set with which to perform free-oscillation research.

The data from the recent events are so numerous and of such high quality that it makes sense to evaluate the current techniques used to analyse split multiplets to make sure we take full advantage of the new recordings. For example, singlet stripping (Ritzwoller *et al.* 1986; Widmer *et al.* 1992) is a useful reconnaissance tool for looking at mode splitting since it gives a rough estimate of singlet frequencies and the overall level of splitting. However, the basic assumption behind singlet stripping—that a multiplet is dominantly sensitive to axisymmetric structure—is very restrictive. Iterative spectral fitting (ISF) (Ritzwoller *et al.* 1986, 1988; Giardini *et al.* 1987,

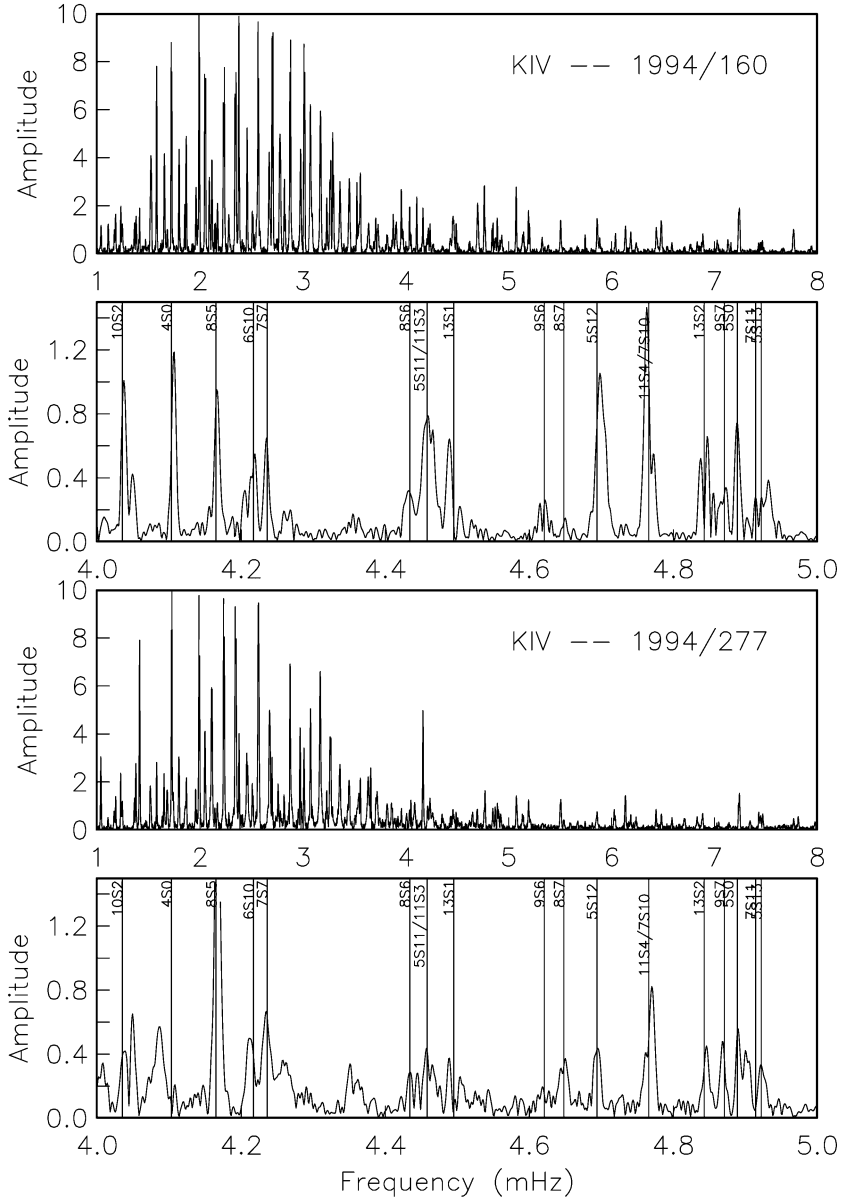

Figure 1. Top two panels show details of a typical spectrum from a vertical-component recording of the Bolivian (1994 June 9) event. 80 hr of data starting 10 hr after the event has been used to emphasize high Q modes, and a linear amplitude scale is used. Note the obvious splitting of some modes (e.g. ${}_{13}S_2$). The bottom two panels show details of a typical spectrum for the Kuril Islands (1994 October 4) event, which is also very overtone-rich.

Table 1. Earthquakes used in this study.

Event name	yyyy.ddd	Depth [km]	Moment [10^{20} N m]	#records	Event code
Balleny Islands Region	1998.084	33	18.2	81	Ba
Fiji	1997.287	166	4.6	88	F2
Flores	1996.169	587	7.3	90	Fl
Irian Jaya	1996.048	33	24.1	103	I
Mexico	1995.282	33	11.5	96	Me
Chile	1995.211	46	12.2	111	C
Kuril Islands	1994.277	54	30.0	101	K
Bolivia	1994.160	631	26.3	88	Bo
Fiji	1994.068	562	3.1	72	F
Macquarie Island	1989.143	10	13.6	52	Ma

1988; Resovsky & Ritzwoller 1998; He & Tromp 1996) avoids this restriction but is very time-consuming and highly non-linear. In fact, ISF often does not converge unless a very good initial solution is available. A major drawback of ISF is that it requires a model of each source used in the mode fitting. For many of the events large enough to excite free-oscillation overtones to observable levels, the sources are complicated and our source models are valid only at relatively long periods. Furthermore, in ISF there is often a trade-off between source mechanism and anelastic structure. Clearly, a new look at the whole issue of splitting-matrix estimation is warranted.

This paper presents a new method for estimating the splitting matrix of an isolated multiplet (or a group of coupled or overlapping multiplets) that circumvents many of the problems described above. The method has some limitations in that it requires at least as many recordings of an earthquake as there are singlets to be analysed. This is rarely a problem with recent data where there are typically 300 or more recordings per event, but it does mean that applying the method to events early in the digital era is problematical unless one confines attention to multiplets of low harmonic degree. Analysing multiplets (or coupled multiplets) of relatively high harmonic degree also requires a large number of events but this becomes less and less of a problem as time proceeds.

THEORETICAL BACKGROUND

For simplicity, we consider the theory for an isolated multiplet—the extension to overlapping and/or coupled multiplets is trivial. Our starting point is the representation of an isolated split multiplet first given by Woodhouse & Girnius (1982) (see also Landau & Lifshitz 1958, section 40):

$$u_j(t) = \sum_{k=1}^{2\ell+1} R_{jk} a_k(t)\, \mathrm{e}^{i\bar{\omega}t} \qquad \text{or} \qquad \mathbf{u}(t) = \mathbf{R}\cdot\mathbf{a}(t)\, \mathrm{e}^{i\bar{\omega}t}\,, \tag{1}$$

where the real part is understood. The jth row of R_{jk} is a $2\ell+1$ vector of spherical harmonics that describe the motion of the spherical-earth singlets at the jth receiver and is readily calculated. $\bar{\omega}$ is the multiplet degenerate frequency and $\mathbf{a}(t)$ is a slowly varying function of time given by

$$\mathbf{a}(t) = \exp(i\mathbf{H}t)\cdot\mathbf{a}(0)\,, \tag{2}$$

where $\mathbf{a}(0)$ is a $2\ell+1$ vector of spherical-earth singlet excitation coefficients that can be computed if the source mechanism of the event is known. $\mathbf{H}$ is the 'splitting matrix' of the multiplet and incorporates all the information about 3-D structure, i.e.

$$H_{mm'} = (a + mb + m^2 c)\delta_{mm'} + \sum \gamma_s^{mm'} c_s^{m-m'}\,, \tag{3}$$

where a, b and c describe the effects of rotation and ellipticity (Dahlen 1968), $\gamma_s^{mm'}$ are integrals over three spherical harmonics that are easy to compute (e.g. Dahlen & Tromp 1998) and the 'structure coefficients', c_s^t, are given by

$$c_s^t = \int \mathbf{M}_s \cdot \delta\mathbf{m}_s^t\, dr\,. \tag{4}$$

$\delta\mathbf{m}_s^t$ are the expansion coefficients of the 3-D aspherical earth structure: $\delta\mathbf{m}(r, \theta, \phi) = \Sigma\, \delta\mathbf{m}_s^t(r)\, Y_s^t(\theta, \phi)$ (which is what we are interested in determining) and $\mathbf{M}_s$ are integral kernels that can be computed (Woodhouse & Dahlen 1978; Woodhouse 1980; Henson 1989).

Receiver strips

Conventional iterative spectral fitting (Ritzwoller *et al.* 1986, 1988; Giardini *et al.* 1987, 1988) proceeds by differentiating eq. (1) with respect to the structure coefficients then iteratively adjusting the c_s^t (or the $\delta\mathbf{m}_s^t$) until a fit to the spectra of all the recording stations is obtained. This is a time-consuming and highly non-linear task. Suppose instead we form the 'receiver strips' for each event:

$$\mathbf{b}(t) = \mathbf{R}^{-1}\cdot\mathbf{u}(t) = \exp[i(\mathbf{H} + \mathbf{I}\bar{\omega})t]\cdot\mathbf{a}(0)\,. \tag{5}$$

This operation is stable since $\mathbf{R}$ is well-conditioned for a typical distribution of stations. (Ill-conditioning of $\mathbf{R}$ would require every station to be at the node of a spherical earth singlet, which is extremely unlikely.)

We actually work in the frequency domain using spectra of Hanning-tapered records in a small frequency band about a multiplet, or group of multiplets, of interest. Some examples of spectra of receiver strips are given in Fig. 2. (Note that these are proportional to the spectra of individual singlets if axisymmetric structure dominates the splitting matrix as is often the case for multiplets that sample the inner core.) Overlapping but uncoupled multiplets of different harmonic degree are often separated by this operation allowing separate estimation of

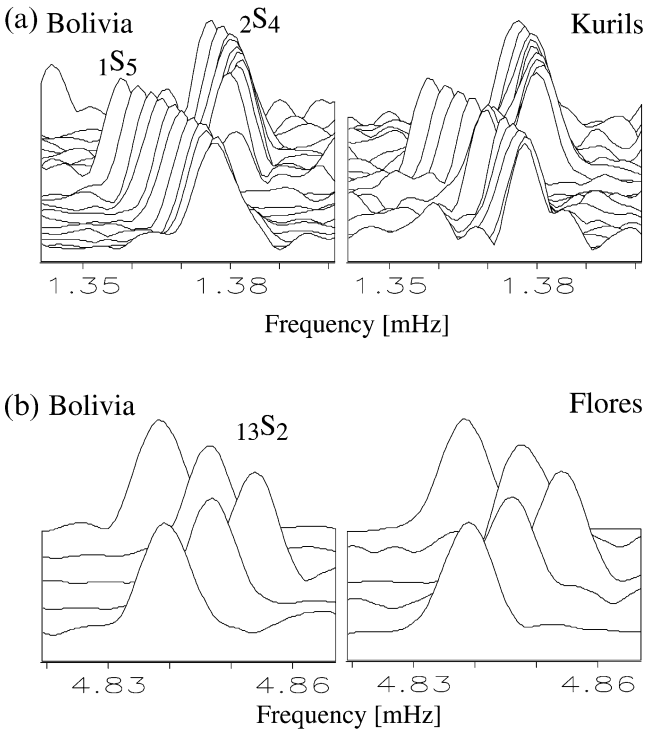

Figure 2. (a) Receiver strips for the overlapping modes $_1S_5$ and $_2S_4$ for the 1994 Bolivian and Kuril Islands events (Table 1). Each strip is a linear amplitude spectrum normalized to unit peak amplitude. The panels show a joint determination of the strips for both modes with the nine strips of $_2S_4$ in the back. A record length of 70 hr was used, which is close to the optimal record length for the faster decaying mode $_1S_5$ (Table 2). The procedure is able to separate the two multiplets effectively. (b) Receiver strips for mode $_{13}S_2$ for the Bolivian and Flores Sea events. A record length of 65 hr was chosen, starting 15 hr after the event time (Table 2). Because $_{13}S_2$ is dominantly split by axisymmetric structure, each strip approximately corresponds to an individual singlet.

their splitting matrices. The receiver strips incorporate all the information about 3-D structure available in the original data but now we have only $2\ell+1$ series (per event) to consider.

Once we have estimates, $\hat{\mathbf{b}}$ say, of the receiver strips, $\mathbf{b}$, we can predict the spectra of individual recordings:

$$\hat{\mathbf{u}} = \mathbf{R} \cdot \hat{\mathbf{b}} .$$

This allows us to check individual recordings and so discard noisy spectra—or even complete events if they did not excite the multiplet of interest. This step also allows us to investigate whether an isolated multiplet is an appropriate model to fit the data. We were able to identify phase errors in some recordings (particularly in the early data) due to either incorrect instrument responses or polarity and timing errors. An example is given in Fig. 3 for the SUR recording of the multiplet ${}_{11}S_4$ excited by the 1977 Tonga event. Such errors are easy to correct by introducing a fictitious time shift. We then recalculate the receiver strips for the selected and/or corrected data of each event and perform a standard linear error propagation (e.g. Jackson 1972) to assign errors to the strips using the residual variance as a measure of data error.

As with ISF, we could now iteratively determine the structure coefficients to fit the spectra of the receiver strips, $\mathbf{b}$. Since this is a highly non-linear procedure and requires knowledge of the source, we suggest an alternative approach that uses the autoregressive nature of the receiver strips. $\mathbf{b}(t)$ satisfies a recurrence in time given by

$$\mathbf{b}(t+\delta t) = \mathbf{P}(\delta t) \cdot \mathbf{b}(t) , \tag{6}$$

where

$$\mathbf{P}(\delta t) = \exp\left[i\left(\mathbf{H} + \mathbf{I}\bar{\omega}\right)\delta t\right] . \tag{7}$$

Note that eq. (6) has no term that depends on the seismic source. If we can recover $\mathbf{P}$ from the data, it is straightforward to obtain $\mathbf{H}$ using an eigenvalue decomposition of $\mathbf{P}$ or a series approximation to the logarithm of $\mathbf{P}$. To recover $\mathbf{P}$, we calculate the spectra of the data, $\mathbf{u}$(t), at different time lags, δt, and then form the receiver strips using eq. (5). We write the spectra of the receiver strips formed from data lagged by $n\delta t$ as $\mathbf{b}_n(\omega)$. Transposing eq. (6) gives a matrix system where each row is a $2\ell+1$ vector of receiver strips at a particular frequency:

$$\begin{bmatrix} \mathbf{b}_{n+1}^{\mathrm{T}}(\omega_1) \\ \mathbf{b}_{n+1}^{\mathrm{T}}(\omega_2) \\ \mathbf{b}_{n+1}^{\mathrm{T}}(\omega_3) \\ \vdots \end{bmatrix} = \begin{bmatrix} \mathbf{b}_{n}^{\mathrm{T}}(\omega_1) \\ \mathbf{b}_{n}^{\mathrm{T}}(\omega_2) \\ \mathbf{b}_{n}^{\mathrm{T}}(\omega_3) \\ \vdots \end{bmatrix} \cdot \mathbf{P}^{\mathrm{T}} \tag{8}$$

or

$$\mathbf{B}_{n+1} = \mathbf{B}_n \cdot \mathbf{P}^{\mathrm{T}} . \tag{9}$$

The phase differences between the n and $n+1$ lags are mainly due to the degenerate frequency of the mode, which is much larger in amplitude than the elements of $\mathbf{H}$. It is therefore best to compute variance reductions as if we were solving the system

$$\mathrm{e}^{-i\omega_g \delta t}\mathbf{B}_{n+1} - \mathbf{B}_n = \mathbf{B}_n \cdot \left[\mathbf{P}^{\mathrm{T}} - \mathbf{I}\right] , \tag{10}$$

where ω_g is an estimate of the degenerate frequency, and the degenerate frequency in eq. (7) is replaced by $\bar{\omega} - \omega_g$. Note that, in the absence of aspherical structure, the left-hand side of eq. (10) is zero so that variance reductions reflect the contribution of 3-D structure.

Eq. (9) can be made overdetermined by stacking receiver strips from different events and, in principle, the signal-to-noise ratio (SNR) can be improved by taking multiple lags and by using multitapers (Thomson 1982). In practice, taking several lags is of only marginal help unless a large amount of time is allowed to lapse between lag pairs so that a different sampling of the noise is achieved. This can be done only at the expense of increasing noise levels in the later lags. On the other hand, stacking receiver strips from different events is crucial since a single event may not excite some of the singlets of a multiplet, or the singlets within a multiplet may be so closely spaced that it may not be possible to take long enough records from a single event to obtain the spectral resolution needed to solve (9). (Exact degeneracy will make $\mathbf{B}_n$ singular for a single event—we explore what constitutes an effective degeneracy in the next section.) Note that stacking events is particularly straightforward since the procedure does not require the source mechanism to be known (thus eliminating a major source of uncertainty present in the iterative spectral fitting technique for large events at high frequencies). In fact, our technique is insensitive to both the temporal and the spatial location of the event and is valid for overlapping events provided the lagged windows include no new sources.

Each row of $\mathbf{B}_n$ and $\mathbf{B}_{n+1}$ in eq. (9) is weighted by the mean frequency-dependent error of the strips deduced from the solution of eq. (5) and the system is solved using a multiple-right-hand-side SVD algorithm (Golub & Reinsch 1971). To avoid potential bias, eq. (9) should really be solved using a method such as total least squares (TLS) or an errors-in-variables (EIV) algorithm (Golub & Van Loan 1983; van Huffel & Vandewalle 1991; van Huffel 1997), although the experiments of the next section indicate that bias is not a significant problem in the examples given here.

The final step is obtaining $\mathbf{H}$ from $\mathbf{P}$. This is most easily done using the eigenvalue decomposition of $\mathbf{P}$, which we compute with the complex Jacobi rotation algorithm COMEIG developed by Eberlein (1970) and described by Wilkinson & Reinsch

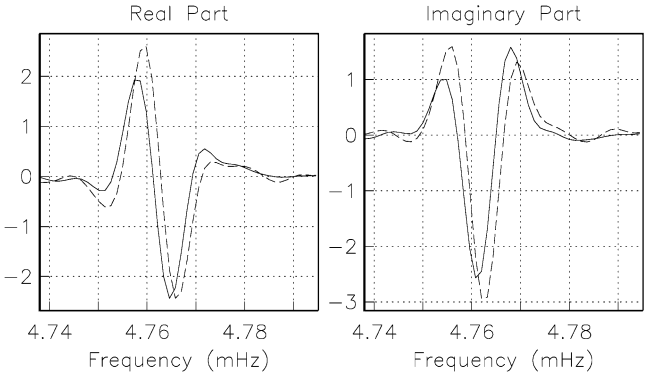

Figure 3. Example of a mismatch between the complex spectra of real data (solid) and predictions (dashed) using the receiver strips of mode ${}_{11}S_4$ for the 1977 June 22 Tonga event recorded at IDA station SUR. The mismatch is due to an inaccurate instrument response that can be modelled by a fictitious frequency-dependent time shift (20 s for mode ${}_{11}S_4$) and a scaling factor.

(1971). We have added to COMEIG the capability to compute left as well as right eigenvectors as suggested by Eberlein. Suppose the decomposition of $\mathbf{P}$ is written as

$$\mathbf{P}(\delta t) = \mathbf{U} \exp[i \boldsymbol{\lambda} \delta t] \mathbf{U}^{-1}, \tag{11}$$

where $\boldsymbol{\lambda} = \boldsymbol{\Omega} + \mathbf{I}(\bar{\omega} - \omega_g)$; then $\mathbf{H} = \mathbf{U}\boldsymbol{\Omega}\mathbf{U}^{-1}$ and our algorithm is essentially complete. Note that we have as yet made no restrictive assumptions about the form of $\mathbf{H}$, so information about anelastic, as well as elastic, structure can be retrieved.

Source strips

It is interesting to note that a similar algorithm can be constructed that uses 'source strips', which might be useful when recordings of a multiplet are available from a large number of well-determined sources, but from relatively few stations. Briefly, we write eq. (1) for the pth source as

$$\mathbf{u}_p(t) = \mathscr{U}(t) = \mathbf{R} \cdot \mathbf{P}(t) \cdot \mathscr{A}_0, \tag{12}$$

where $\mathscr{A}_0 = \mathbf{a}_p(0)$. For a sufficiently large number of well-determined sources, the matrix $\mathscr{A}_0$ will be well-conditioned and its inverse can be found, allowing us to construct $\mathscr{V}(t) = \mathscr{U}(t)\mathscr{A}_0^{-1}$. In index notation we can compute

$$\mathscr{V}_{jk}(t) = R_{nj} \exp(i[H_{nk} + \delta_{nk}\bar{\omega})t]. \tag{13}$$

For each record-station index, j, $\mathscr{V}_{jk}(t)$ is a 'source strip' that has the AR property

$$\mathscr{V}(t + \delta t) = \mathscr{V}(t) \exp[i(\mathbf{H} + \mathbf{I}\bar{\omega})\delta t],$$

which again allows recovery of $\mathbf{H}$ in an analogous fashion to the previous section. This particular algorithm is not in general as attractive as the use of receiver strips since it requires good models of many earthquake sources, and it could conceivably fail if a single receiver does not record all of the singlets. However, it may be useful for analysing splitting matrices using many recordings from an extremely high-quality station. An example would be the Black Forest Observatory (BFO), where barometric pressure has been recorded for many years allowing corrections for atmospheric gravitational attraction to be applied to high-quality gravimeter recordings (Zürn & Widmer 1995). This process results in extremely high SNR recordings of very long-period spheroidal mode multiplets.

Decomposing the splitting matrix

The splitting matrix can be inverted for 3-D structure directly but it is also useful to determine structure coefficients and so-called 'splitting functions'. If we think of structure as having a real (elastic) and imaginary (anelastic) part, we can use the unique representation

$$\mathbf{H} = \mathbf{E} + i\mathbf{A}, \tag{14}$$

where $\mathbf{E} = (\mathbf{H} + \mathbf{H}^{\mathrm{H}})/2$ and $i\mathbf{A} = (\mathbf{H} - \mathbf{H}^{\mathrm{H}})/2$ and superscript H indicates Hermitian transpose. Both $\mathbf{E}$ and $\mathbf{A}$ are Hermitian and can be written:

$$E_{mm'} = \sum_s \gamma_s^{mm'} c_s^{m-m'}; \qquad A_{mm'} = \sum_s \gamma_s^{mm'} d_s^{m-m'}, \tag{15}$$

where we have removed the effects of rotation and ellipticity. The γs are the geometrical factors of eq. (3), the c_s^t are the elastic structure coefficients, and the d_s^t are the anelastic structure coefficients. Regarding eq. (15) as a pair of linear inverse problems for $\mathbf{c}$ and $\mathbf{d}$ is beneficial as it allows us to include explicitly penalties for rough structure (i.e. high s) and so remove structure that is not required to fit the data. It is also interesting to note that there are exact transformations relating structure coefficients to splitting matrix elements (Giardini *et al.* 1988; Gilbert & Woodhouse 2000) but we have not used these in this work.

Finally, it is convenient to visualize structure sensed by a multiplet by forming the elastic splitting function (Woodhouse & Giardini 1985),

$$F_{\mathrm{E}}(\theta, \phi) = \sum_{s,t} c_s^t Y_s^t(\theta, \phi), \tag{16}$$

and an equivalent function for anelastic structure where the c_s^t are replaced by d_s^t.

Extension to coupled multiplets

The extension to coupled multiplets is straightforward. Eqs (1) and (2) have the same form as before but now the rows of $\mathbf{R}$ include the displacements of all singlets that are coupling together. Suppose two multiplets couple, the first with harmonic degree ℓ_1 and the second with harmonic degree ℓ_2. The total number of columns of $\mathbf{R}$ is $2(\ell_1 + \ell_2 + 1)$, with the first $2\ell_1 + 1$ elements of each row corresponding to the displacements of the singlets of multiplet 1 and the last $2\ell_2 + 1$ elements corresponding to the displacements of the singlets of multiplet 2. In a similar fashion, $\mathbf{a}(0)$ consists of the two source vectors for multiplet 1 and multiplet 2 concatenated together, and $\bar{\omega}$ is replaced by an arbitrary fiducial frequency between the degenerate frequencies of the coupling multiplets. The splitting matrix, $\mathbf{H}$, now has a block form,

$$\begin{bmatrix} H_{11} & H_{12} \\ H_{21} & H_{22} \end{bmatrix},$$

where the self-coupling blocks, H_{11} and H_{22}, are identical to the splitting matrices of the multiplets as if they were uncoupled. In particular, their traces give the difference between the fiducial frequency and the degenerate frequencies that the multiplets would have if the Earth were spherically symmetric—the diagonal-sum rule of Gilbert (1971). Such data are useful for modelling the terrestrial monopole. Note that it is unnecessary to consider the coupling multiplets as a 'supermultiplet' and apply the diagonal-sum rule to it as was first suggested by Woodhouse (1980).

The coupling blocks, H_{12} and H_{21}, are also retrieved in the procedure described above and each can be described by a set of structure coefficients in a manner analogous to eq. (3). The interesting thing about these blocks is that the coupling provides sensitivity to structure of odd harmonic degree. Coupled multiplets have already been studied using a generalization of ISF by Resovsky & Ritzwoller (1995, 1998).

APPLICATIONS

In this section, we show examples of retrieving the splitting matrix, $\mathbf{H}$, for both synthetic and real data. Synthetic data are calculated for each observed recording and serve as input data in a test inversion. The synthetics are calculated using the coupled-mode code of Park & Gilbert (1986). Rotation of

the earth, ellipticity and elastic upper mantle model M84A (Woodhouse & Dziewonski 1984), but no 3-D attenuation, are included in the calculations.

We apply the algorithm described in the earlier sections, using the following recipe.

(1) Calculate $\mathbf{R}$ and $\mathbf{R}^{-1}$ (eqs 1 and 5) for each event.
(2) Calculate spectra of seismograms for selected time lags $n\delta t$.
(3) Calculate receiver strips, $\mathbf{b}_n(\omega)$, for each event and lag index n.
(4) Choose a frequency band in which the receiver strips have significant amplitude for the multiplet(s) being analysed.
(5) Compose matrices $\mathbf{B}_n(\omega)$ (eqs 8 and 9). The matrices have $2\ell+1$ columns (for a single multiplet), and the row dimension # stations × # events × # frequencies. The row dimension can be increased by taking multiple lags.
(6) Solve eq. (9) for $\mathbf{P}^{\mathrm{T}}$, e.g. using MINFIT (Golub & Reinsch 1971) or a TLS/EIV algorithm (e.g. van Huffel 1997).
(7) Decompose $\mathbf{P}$ (using COMEIG) (eq. 11) and construct $\mathbf{H}$.

All spectra are computed using a taper or 'window' to reduce spectral leakage. Application of a taper reduces bias by interference from neighbouring multiplets at the expense of reducing local spectral resolution. In mode analyses, good spectral resolution is extremely important so our choice of tapers is limited. The spectral smoothing characteristics of a taper are often discussed in units of a Rayleigh bin ($=2\pi/T$ rad s^{-1}, where T is the record length). A boxcar window has the best resolution (0.89 Rayleigh bins) but has very bad spectral leakage characteristics. In this paper, a Hanning taper is used that has a resolution of 1.44 Rayleigh bins and moderate resistance to spectral leakage (Harris 1978). More sophisticated tapers could be used, including multitapers (Thomson 1982; Lindberg & Park 1987), although the time–bandwidth product must be chosen to be small to attain useful spectral resolution, and little is gained over using a more conventional single taper.

We have experimented with varying the time lag, δt, and find that our results are remarkably insensitive to the choice of this parameter, provided it is larger than about 1/3 of the period of the mode. The choice of record length has also been the subject of some experiment. When analysing a single decaying sinusoid in the presence of noise and using a Hanning taper, Dahlen (1982) has shown that roughly Q cycles of data should be taken to give optimal frequency estimation. Here, we are trying to resolve beating between singlets of a multiplet, which requires much better spectral resolution, suggesting that we should take longer records. Clearly, the optimal record length will also depend on the degree of splitting of the multiplet—a multiplet that shows little splitting will need longer records than a more broadly split multiplet. Of course, the SNR will decrease as we take longer records, so there is the usual trade-off between spectral resolution and SNR.

We examine the problem with an analysis of the multiplet ${}_4S_1$ using synthetic data. This multiplet has three relatively coarsely spaced singlets that, in the theoretical model, span a frequency band of 8 μHz. The energy of the multiplet is smeared over a broader frequency band by the process of tapering, although the degree of smearing depends upon the record length. We are able to recover $\mathbf{H}$ of ${}_4S_1$ using only one event if we use 100 or more hours of data. This record length corresponds to a spectral averaging length of about 4 μHz (when using the Hanning taper). Thus, we find that we can recover $\mathbf{H}$ when the number of independent spectral estimates that spans the taper-broadened multiplet equals or exceeds the number of singlets within the multiplet (in this case, three). With real data, taking 100 hours leads to noisy strips and, if we use about Q cycles of data, we need two or more events to obtain a stable estimate of $\mathbf{H}$.

We also expect that the number of events needed to resolve the splitting matrix of a multiplet will depend on the degree of degeneracy of the multiplet. We illustrate the problem with mode ${}_{22}S_1$ with two cases. In the first case, we include only ellipticity so that the ± 1 lines are exactly degenerate and the total splitting width is about 10 μHz. We find that, as expected, we are unable to recover the splitting matrix using one event for any record length, although using two events together allows $\mathbf{H}$ to be recovered. Including the mantle model M84A splits the ± 1 lines by only 0.2 μHz and we find that we can now recover the splitting matrix using one event and a record length that gives three independent spectral estimates spanning the taper-broadened multiplet (about 2 Q cycles). This ability to resolve splitting matrices in the presence of near-degeneracy is not confined to $\ell=1$ multiplets. For example, ${}_4S_4$ has nine singlets, six of which are extremely closely spaced in frequency, yet we are able to recover the splitting matrix using only three events with a record length of about 3 Q cycles. Of course, with real data we cannot take such long records without being swamped by noise, but four or five events are still sufficient when taking only Q cycles.

Examples with synthetic data

Example 1: An isolated multiplet

To illustrate the strengths of the AR method, we show the results of a series of tests with a multiplet (${}_5S_3$) that is mainly sensitive to shear velocity structure in the mantle, especially in the upper mantle. Our tests start with the assumption that ${}_5S_3$ is a well-isolated multiplet, that is, there is no interfering mode nearby. The spectra of individual records are calculated using the same taper (Hanning) we use for the real data with record lengths of about Q cycles (Table 2).

We begin by inverting for the splitting matrix using events Bo, K and F (Table 1) and add more events until the output splitting matrix is sufficiently close to the input matrix. Fig. 4(a) shows that three events do not provide enough constraints to recover even the singlet frequencies. As more events are added, the retrieval of the singlet frequencies and $q(=1000/Q)$ improve. A combination of four events provides satisfactory recovery of the complex singlet frequencies, but the off-diagonal elements of the output splitting matrix poorly represent those of the input matrix (Fig. 4b). The recovery of the full splitting matrix requires at least seven events (Table 2).

We assess the quality of the process numerically by comparing the mean deviation σ of the matrix elements between input and output matrix:

$$\sigma = \sqrt{\frac{1}{N}\sum_{N} |H(i,j) - H_0(i,j)|^2},$$

where H_0 is the input matrix, H is the output matrix and $N=(2l+1)^2$. Fig. 4(c) shows σ as a function of number of events taken. The recovery improves as more events are added,

Table 2. Parameters of the modes used in this study.

Mode name	Frequency (PREM) [mHz]	q (PREM) $(1000/Q)$	Estim. Q-cycles [hr]	Start time [hr]	Record length [hr]	Frequency(†) band	Events (synth)	Events (data)
${}_5S_3$	2.16966	3.420	40	1	45	2.155–2.185	Bo,K,Fl,I,Ba,F,C	–
${}_4S_4$	2.27960	3.446	40	1	45	2.268–2.289	Bo,K,Ma,Me,I	all but C,Ba, or all
${}_1S_5$	1.37027	3.426	65	1	70	1.355–1.380	Bo,K,Fl,I	all but F2,F
${}_2S_4$	1.37920	2.630	80	1	70	1.374–1.386	Bo,K,Fl,I,Ba,F,C	all but F
${}_2S_4/{}_1S_5$	–	–	–	1	70	1.355–1.386	all events	all events
${}_{10}S_2$(*)	4.03233	5.217	40	10	75	4.030–4.055	Bo,K,Fl,I	all but I,Me,Ma
${}_{13}S_2$	4.84526	1.138	55	15	65	4.835–4.860	Bo,K,F,I,Ba	all but I,Me,Ma
${}_8S_1$	2.87336	1.075	100	25	90	2.868–2.879	Bo,K,Fl	Bo,K,F2,C,Ba,Fl
${}_{13}S_1$	4.49573	1.360	50	15	65	4.485–4.508	Bo,K,Fl	Bo,K,F2,C,Fl,F

Q-cycles are estimated using the mean predictions of a variety of models.
(*) Q-cycles for ${}_{10}S_2$ are somewhat uncertain since the eigenfunctions depend on the 1-D earth model.
(†) Frequency band chosen in the inversion of the receiver strips for the splitting matrix.

although there is little improvement after eight events. The greatest improvement actually comes between using three and four events (not shown).

Performing many experiments of this type leads us to the relatively conservative rule of thumb that $2\ell+1$ events is a reasonable choice for the number of events when using record lengths of about Q cycles. As noted above, we might be able to lower this number by taking longer record lengths; the improvement is illustrated in Fig. 4(c) for a record length of 60 hr. In practice, the presence of noise limits the improvement obtained by taking a longer record (see below).

Also shown in Fig. 4(a) are the results obtained from a singlet stripping analysis. Each strip ideally corresponds to a single Y_ℓ^m and is not a true singlet unless the perturbing structure sensed by the multiplet is axisymmetric. Model M84a has significant non-axisymmetric structure (as sensed by ${}_5S_3$) so that each 'singlet strip', for a single Y_ℓ^m, is a combination of two or more true singlets. To be more precise, we shall use the term m-singlet for a Y_ℓ^m strip, and the term ω-singlet for a true singlet. Interference between the singlets means that the apparent frequencies and qs measured from the m-singlet strips deviate from the true ω-singlet complex frequencies. It follows that complex degenerate frequencies estimated from the means of m-singlet strip apparent frequencies can also be biased. For example, the AR method gives a degenerate frequency and mean q that are correct to within 0.005 μHz and 0.002 respectively but m-singlet stripping gives values that are only correct to within 0.02 μHz and 0.2.

Example 2: bias introduced by random noise

The next example shows the effects of incoherent noise on the estimation of the splitting matrix. We add Gaussian noise to each of the seismograms with a variance that is 3 per cent of the maximum amplitude in each time series (the synthetics are composed mainly of the first five overtone branches with harmonic degree up to $\ell=8$). For a record length of 45 hr, the SNR for the spectral peak of ${}_5S_3$ varies between 0.5 and 15 (the mean SNR ratio is 6 : 1), which is typical for an average event in our data set, although much noisier than our best events.

Incoherent noise degrades the recovery but adding more events to the inversion can overcome much of the degradation. The complex singlet frequencies and the major features of the splitting matrix can be recovered quite accurately if we take nine events (compare Figs 5 and 4b). It is also true that choosing a longer record length or taking more than nine events does not significantly alter the result of the inversion (that is, there is no improvement and no further degradation).

In the presence of noise, the inversion for **P** (and hence the determination of **H**) is greatly stabilized by weighting by the errors assigned to the receiver strips. Formally, the standard error propagation provides different error bars for each of the $2\ell+1$ receiver strips that are a function of frequency. Since we solve for **P** using a multiple right-hand side SVD, we average the errors over all singlets, at each frequency, for each event, and assign this value to all receiver strips. This process diminishes the influence of noisy strips that are usually caused by poor multiplet excitation by a particular event. This weighting by event, which is important in this example but much more so in the next one, dramatically reduces the dependence of the results on the subjective choice of the frequency band in which the fitting is to be done. A more thorough treatment of errors requires the use of a TLS or EIV approach and will be the subject of future work.

Example 3: bias introduced by mode interference

In the previous test, we assumed that ${}_5S_3$ could be regarded as a well-isolated multiplet. The nearest neighbours are about 20 μHz away on one side (${}_1S_{10}$) and 60 μHz on the other side (cluster ${}_0S_{14}$, ${}_7S_1$, ${}_2S_9$). In spectra of individual records of real data, the spectral amplitude of this multiplet is typically rather small. In fact, the amplitude of ${}_5S_3$ is often just 10 per cent of that of the neighbouring fundamental modes ${}_0S_{13}$ and ${}_0S_{14}$. It is also true that ${}_1S_{10}$ sometimes causes peaks of significant amplitude to appear in the receiver strips of ${}_5S_3$, if ${}_1S_{10}$ is ignored (e.g. synthetic example in Fig. 6a for event Bo). The relatively high attenuation of ${}_5S_3$ relative to ${}_1S_{10}$ does not allow us either to choose significantly longer time windows or to start later in the record to reduce interference effects. In this case, it is advisable to include ${}_1S_{10}$ in the receiver strips.

We include ${}_1S_{10}$ in the synthetic seismograms and use the same time-series length as before (45 hr) and the same frequency band (2.155–2.185 μHz) to determine the splitting matrix of ${}_5S_3$. Fig. 6(b) clearly shows that the recovery of the

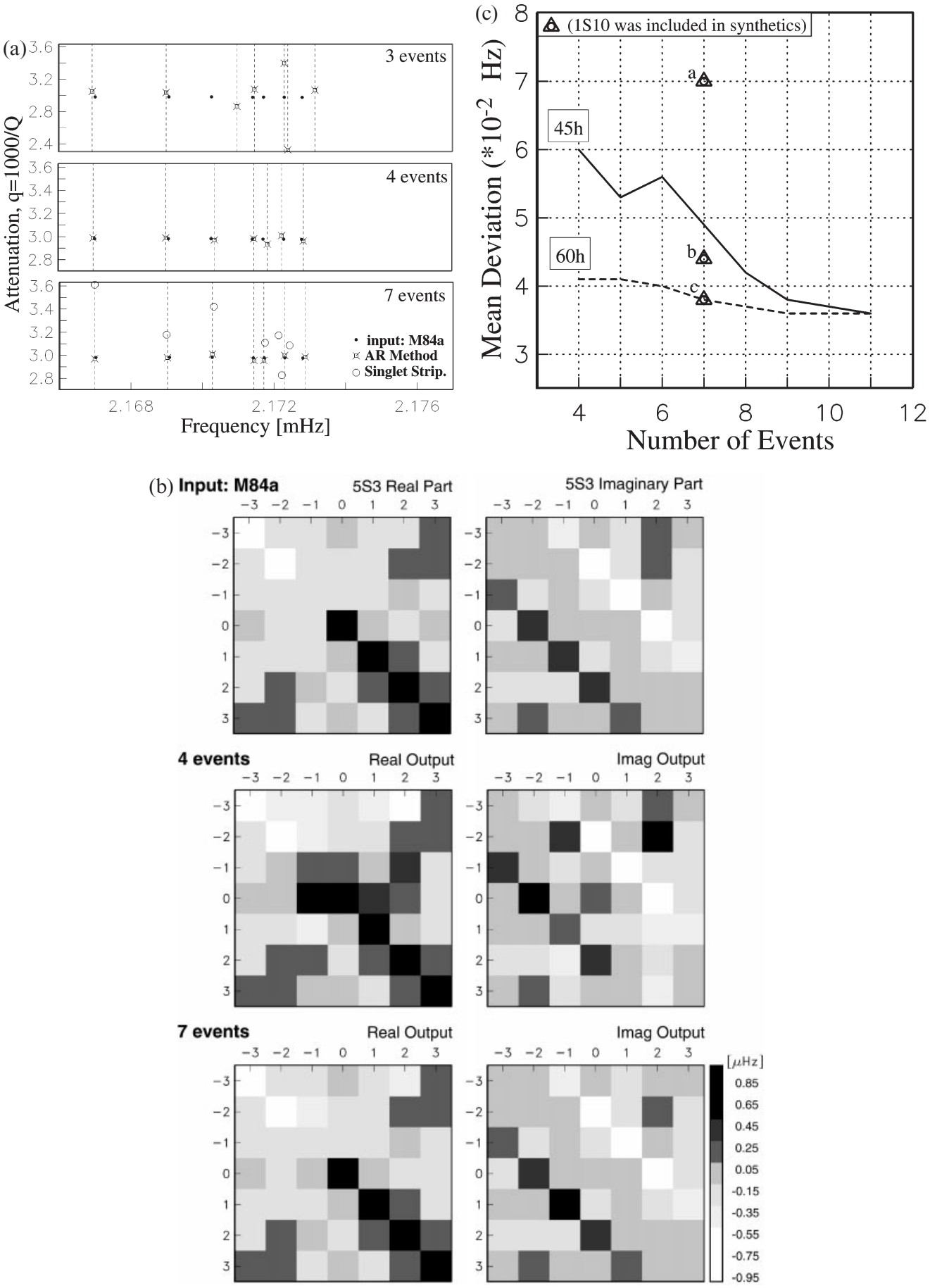
(a)
3 events
4 events
7 events
Attenuation, q=1000/Q
Frequency [mHz]
input: M84a
AR Method
Singlet Strip.
(c)
(1S10 was included in synthetics)
45h
60h
a
b
c
Mean Deviation (*10-2 Hz)
Number of Events
(b) Input: M84a
5S3 Real Part
5S3 Imaginary Part
4 events
Real Output
Imag Output
7 events
Real Output
Imag Output
[μHz]
0.85
0.65
0.45
0.25
0.05
-0.15
-0.35
-0.55
-0.75
-0.95

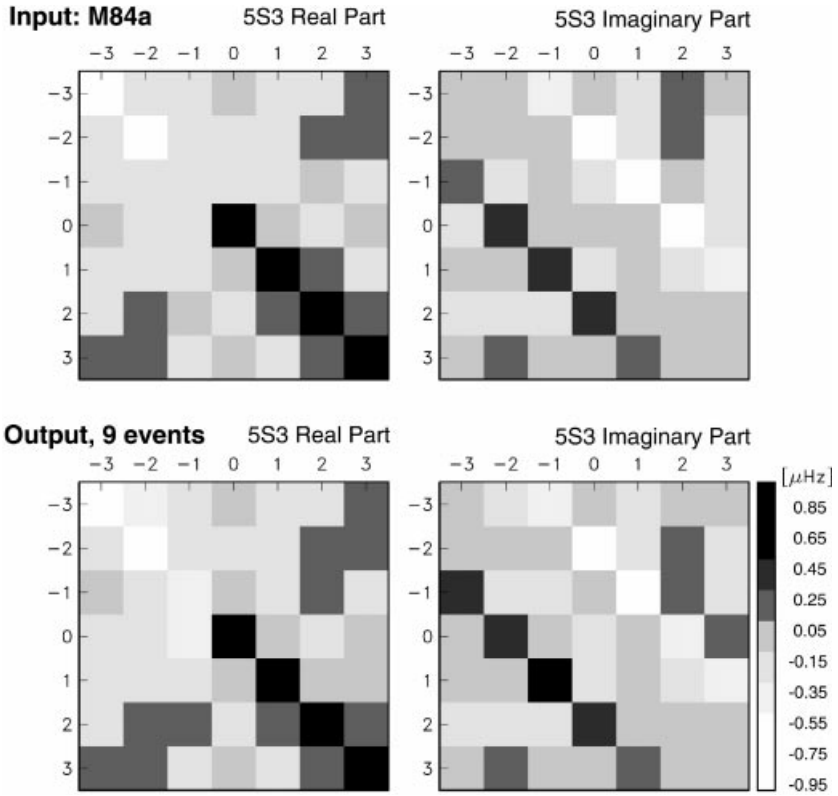

Figure 5. Recovery of the splitting matrix of mode ${}_5S_3$ using synthetic data for the case when 3 per cent Gaussian noise is added to the synthetic seismograms. This example shows the recovery using nine events (Table 2, plus Me and F2).

splitting matrix fails if we ignore ${}_1S_{10}$ in the determination of the receiver strips. Even the singlet frequencies are retrieved with significant errors (not shown). Including ${}_1S_{10}$ in the calculation of the receiver strips, and then determining the splitting matrix for ${}_5S_3$, using only those receiver strips associated with ${}_5S_3$, provides a marked improvement (Figs 6b and 4c). The splitting matrix is now recovered with high accuracy.

Unfortunately, it is very often the case that not enough records are available per event to include all possible interfering modes in the calculation of the receiver strips (at least $2\ell+1$ records for each multiplet). This is especially true for events occuring before about 1988. Very often the choice of a longer record length improves the ability to separate interfering multiplets without having to include them explicitly in the analysis. For example, using a record length of 60 hr instead of 45 hr is indeed very competitive to the strategy of including the interfering multiplet ${}_1S_{10}$ in the receiver strips (Fig. 4c).

Example 4: an overlapping mode pair

Our last test shows that we are able to estimate the splitting matrices for significantly overlapping and coupled multiplets, using as an example the pair ${}_1S_5/{}_2S_4$. The synthetic data include coupling between the multiplets due to M84A. Fig. 7(a) shows the receiver strips for the synthetic data for the Bolivian event. We choose a window length of 70 hr, which is close to Q-cycles of the more attenuating mode (Q-cycles are 65 hr for ${}_1S_5$ and 80 hr for ${}_2S_4$). The receiver strips are determined including both multiplets simultaneously, and recovery of the joint splitting matrix is performed using all 10 events, although taking fewer events yields rather similar results. Fig. 7(b) compares input and output singlet frequencies while Fig. 7(c) compares the input and output splitting matrices. The recovery of the complex singlet frequencies is very accurate and the off-diagonal coupling blocks are faithfully recovered by the method as well as the diagonal self-coupling blocks.

Figure 4. (a) Recovery of the frequencies and q of mode ${}_5S_3$ using synthetic data for the first three, the first four and all seven events of Table 2. Both frequency and q of all singlets are recovered when using seven events. For three events, we recover only four frequencies and two values of q correctly. The dashed lines are guides that are aligned with the singlet frequencies determined with the AR method. Also shown are the results from m-singlet stripping. These results are clearly biased as they cannot account for the effects introduced by non-axisymmetric structure. (b) Recovery of the splitting matrix of mode ${}_5S_3$ for synthetic data using the first four and all seven events of Table 2. While four events clearly cannot constrain the splitting matrix, seven events provide a satisfactory recovery. (c) The mean deviation of the matrix elements between input and output matrix as a function of number of events used in the inversion. The recovery improves as more events are taken. Curves for two record lengths (45 and 60 hr) are shown. The longer record length provides better spectral resolution and, hence, a better fit for the same number of events. Shown by triangles are the mean deviations for the case when mode ${}_1S_{10}$ is included in the synthetic seismograms. (a) ${}_1S_{10}$ is ignored in the receiver strips, record length is 45 hr; (b) ${}_1S_{10}$ is ignored, record length 60 hr; (c) ${}_1S_{10}$ is included in the strips, record length 45 hr.

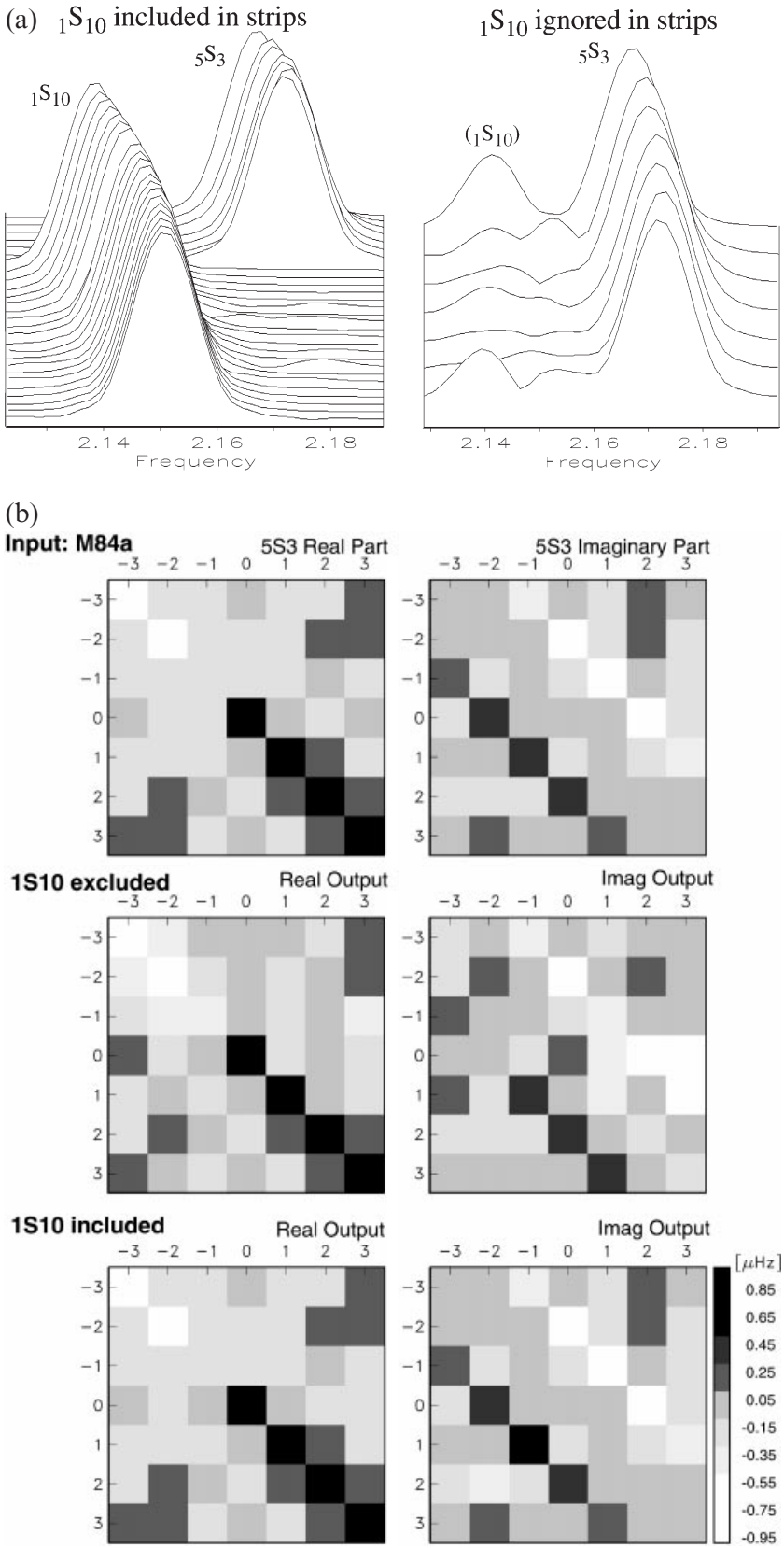

Figure 6. (a) Receiver strips from synthetic data of the Bolivian event for the case when $_1S_{10}$ is included in the synthetics and in the calculation of the receiver strips (left) and for the case when $_1S_{10}$ is included in the synthetics but ignored when calculating the receiver strips for $_5S_3$ (right). Low-amplitude spectral peaks appear near the frequency of $_1S_{10}$ in the latter case. (b) Recovery of the splitting matrix of mode $_5S_3$ using synthetic data for the case when $_1S_{10}$ is present in the synthetics. (Top) input matrix; (middle) recovered matrix ignoring $_1S_{10}$ and using seven events; (bottom) recovered matrix including $_1S_{10}$ in the calculation of the receiver strips but using only those strips of $_5S_3$ for the inversion of the splitting matrix.

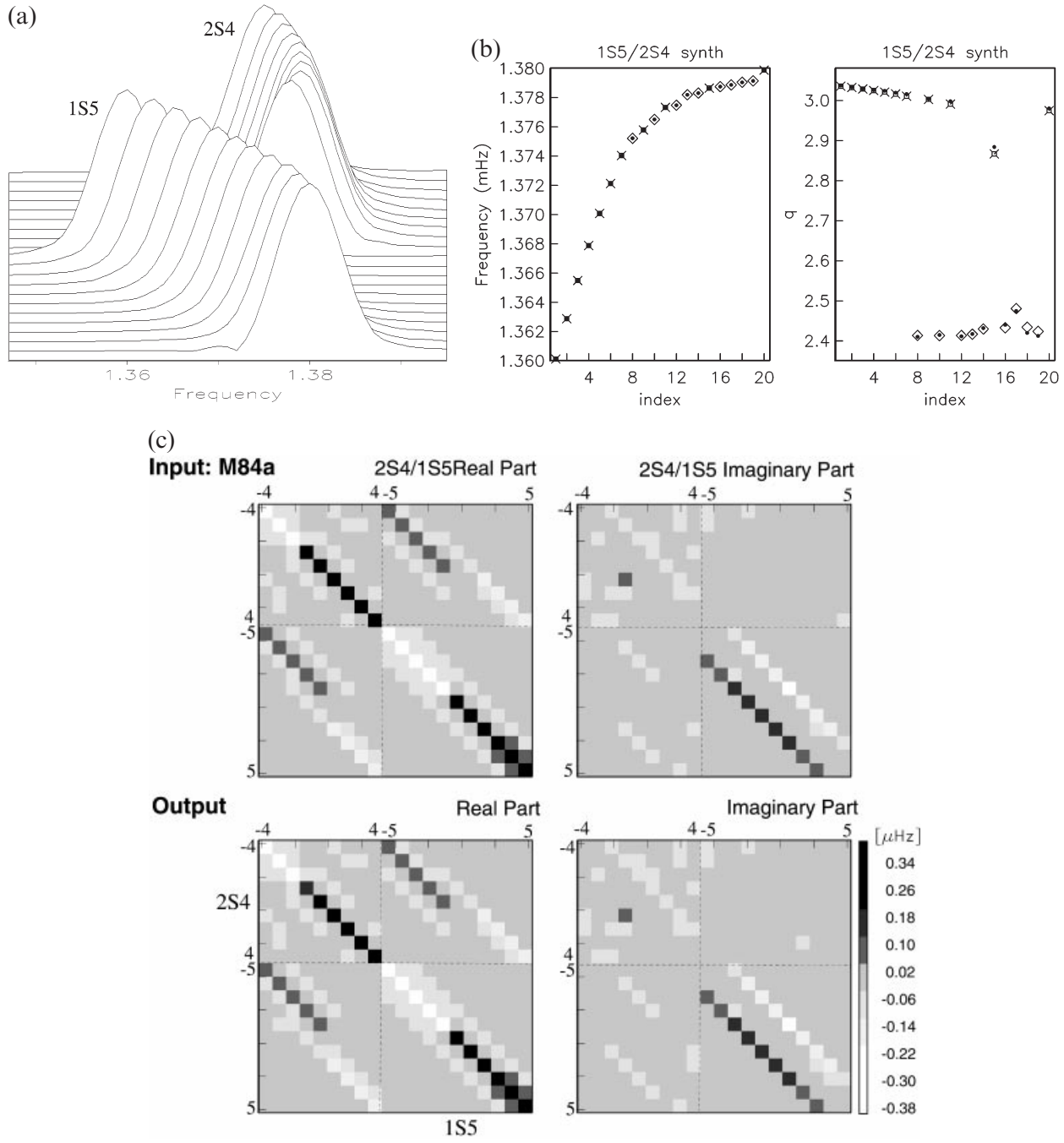

Figure 7. (a) Receiver strips from synthetic data of the Bolivian event for mode pair ${}_1S_5/{}_2S_4$. A record length of 70 hr was chosen to calculate the strips. (b) Recovered frequencies and qs for the singlets of the coupled mode pair ${}_1S_5/{}_2S_4$. The frequencies of the pair are sorted by increasing value. The dots denote the recovered values, the crosses indicate the theoretical values for ${}_1S_5$, and the diamonds indicate the theoretical values for ${}_2S_4$. (c) The combined splitting matrix of mode pair ${}_2S_4/{}_1S_5$. The upper two panels show the input matrix and the lower two panels show the output matrix. The upper and lower diagonal blocks are those of modes ${}_2S_4$ and ${}_1S_5$ respectively and are practically identical to the results of inversions performed for both modes separately. The off-diagonal coupling blocks are also well recovered.

In all of the above tests, we have used a simple SVD to solve eq. (9) with the implicit assumption that $\mathbf{B}_n$ is error-free. To test that this does not lead to bias, we verified that we obtain identical results by interchanging $\mathbf{B}_{n+1}$ and $\mathbf{B}_n$ in eq. (9). We find that $\mathbf{P}$ is recovered as before but, of course, with a negative time lag.

Summary

The main result of these tests is that the method can always be made to work if enough events are available. As a rough rule of thumb, taking at least as many events as singlets is sufficient but, in many cases, fewer events will suffice (for example, event

Bo is enough to retrieve the frequencies of ${}_{13}S_1$, whose splitting matrix is strongly diagonally dominant). The effects of interference with neighbouring multiplets that are ignored in the calculation of the receiver strips can sometimes be reduced by taking records longer than Q-cycles, although including the neighbouring multiplet in the calculation of the receiver strips is preferable (if enough records per event are available). Finally, the inversion for splitting matrices of overlapping but uncoupled multiplets is successful without significant mapping from one multiplet self-coupling block into the other or into the cross-coupling blocks. This implies that the method will be successful in retrieving the complete splitting matrix of coupled multiplets.

Real data

With real data, the splitting matrix is generally non-Hermitian due to the 3-D variation of anelastic structure within the Earth. The effects of elastic and anelastic structure can be formally separated using the decomposition described by eq. (14). 'Noisy' receiver strips will cause some of the elastic structure to be mapped into anelastic structure and vice versa. For example, the output matrices in the synthetic tests are slightly non-Hermitian even though a 1-D attenuation model was used to calculate the synthetic seismograms. In our synthetic tests, such erroneous mapping is rather small provided enough events are taken. In fact, the maximum value in matrix **A** (anelastic part) is rarely greater than the minimum value of matrix **E** (elastic part). With real data, we find that taking many events improves the SNR and reduces cross-talk between **A** and **E** (see below). This leads us to believe that we can obtain unbiased estimates of both elastic and anelastic splitting matrices.

Example 1: an isolated mantle multiplet

Our first example using real data is ${}_4S_4$, which is primarily sensitive to shear velocity in the mantle. This multiplet is fairly well isolated, with its spheroidal mode neighbours being roughly 50 μHz away on one side (${}_0S_{14}$) and 65 μHz on the other (${}_0S_{15}$). All three multiplets attenuate at approximately the same rate (Q-cycles are roughly 40 hr). If we use a record length of 45 hr, synthetic tests show that we can retrieve the splitting matrix using five events (see Table 2). We have chosen these events because their receiver strips for real data have the highest SNR. When inverting the real data, we find that more events are necessary to obtain a stable result. A set of eight events (Table 2) yields stable estimates of the complex singlet frequencies but some elements of the splitting matrix are still rather large, especially those in the anelastic part, **A**. Such elements usually disappear when adding more events. Fig. 8 illustrates the splitting matrix of ${}_4S_4$ obtained using all 10 events.

To compare our results for the elastic part of the splitting matrix with those of other authors, we remove the effects of rotation and ellipticity from the diagonal, determine the structure coefficients (eq. 15) and calculate splitting functions (eq. 16). The inversion for the structure coefficients finds the

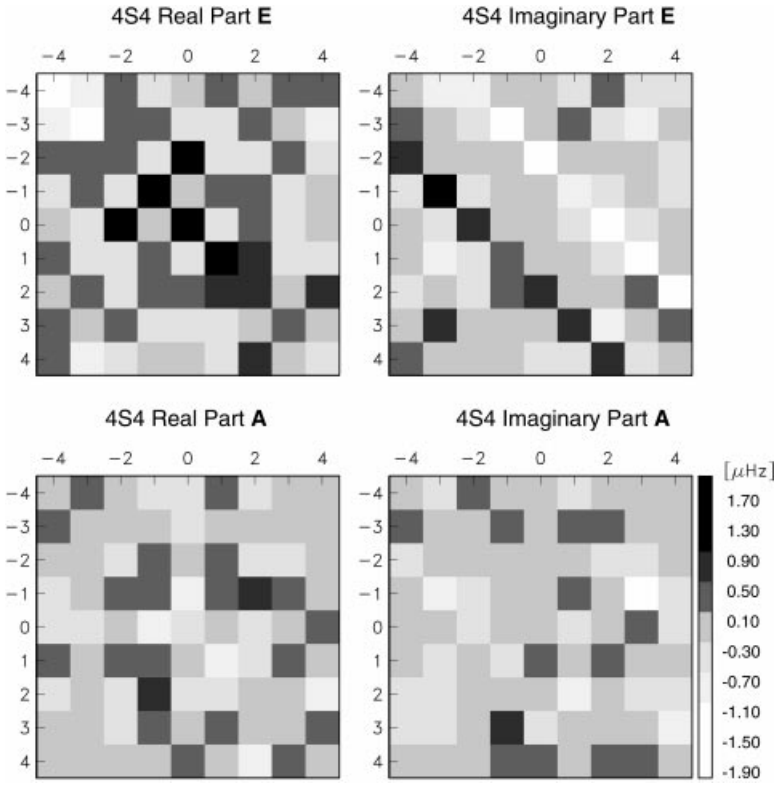

Figure 8. Splitting matrix for mode ${}_4S_4$ obtained using real data from all 10 events of Table 1. The upper two panels show real and imaginary parts of **E** (eq. 14) while the lower two panels show **A**. The elastic part, **E**, is dominated by two bands in the imaginary part for $m-m'=2$. Note that the anelastic part is significantly smaller than the elastic part.

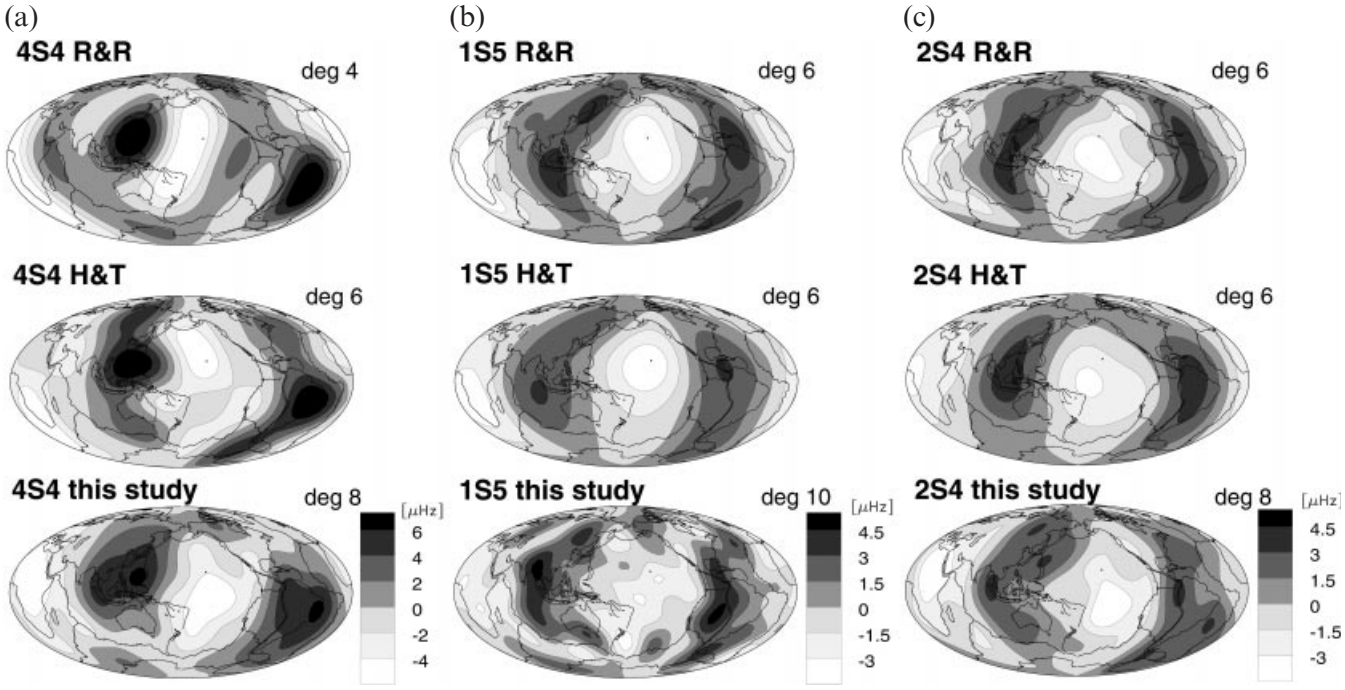

Figure 9. Elastic splitting functions for three modes obtained using eq. (16): (a) ${}_4S_4$, (b) ${}_1S_5$, (c) ${}_2S_4$. The effects of rotation and ellipticity have been removed prior to the inversion for structure coefficients. For comparison, the splitting functions of other authors are also shown: R&R—Resovsky & Ritzwoller (1998); H&T—He & Tromp (1996). The maximum harmonic degree included in each splitting function is indicated for each map.

smoothest splitting function that statistically fits the splitting matrix elements. [Note that we use a delete-one jackknife procedure (Efron 1982) on our 10 earthquakes to assign errors to **H**.] Fig. 9(a) compares our splitting function with those of Resovsky & Ritzwoller (1998) (hereafter R&R) and He & Tromp (1996) (hereafter H&T). The agreement between the maps is quite good, although it should be noted that each study has a different spherical harmonic cut-off in the splitting function (see figure caption). The correlation of the R&R map with either of the others is significantly less than that between the two other maps (Table 3), and the correlation coefficient between our map and the R&R map is below the 99 per cent confidence level. The disagreement is mainly due to the fact that the R&R map has structure in degree 4 that is almost as large as the degree 2 structure. Such behaviour is not predicted by any current models of mantle structure and is absent in the other two maps.

Example 2: the multiplet pair ${}_1S_5/{}_2S_4$

Our next example is the overlapping pair ${}_1S_5/{}_2S_4$. As in the synthetic test, we choose a record length of 70 hr to calculate the receiver strips of both multiplets simultaneously. For mode ${}_1S_5$, taking four events (Bo, K, I, Ba) constrains the basic structure of the entire splitting matrix, although significant improvement is achieved by adding more events. The splitting matrix obtained using four events is somewhat noisy in the sense that individual matrix elements, especially the elements for **A** at the edges (i.e. $m, m' = \pm 4$), can be rather large. The fact that these elements are greatly diminished by adding more events indicates that they are not initially well constrained. We add events successively until the splitting matrices no longer change significantly. Our optimal choice includes eight events (all from Table 1 except for the two Fiji events). For ${}_1S_5$, the anelastic part appears to be significant as the average size of

Table 3. Correlation of splitting functions of various authors.

Mode name	Harm. deg. used	Corr. MLG–RR	Corr. MLG–HT	Corr. RR–HT	Corr. MLG–Li	Corr. HT–Li	99% conf.
${}_4S_4$	2,4	0.65	0.84	0.74	–	–	0.66
${}_1S_5$	2,4,6	0.73	0.80	0.90	–	–	0.50
${}_2S_4$	2,4,6	0.86	0.80	0.92	–	–	0.50
${}_8S_1$	2	0.98	0.88	0.89	–	–	0.92
${}_{13}S_2$	2,4	–	0.79	–	0.94	0.79	0.66
${}_{10}S_2$	2,4	–	–	–	0.82	–	0.66
${}_{13}S_1$	2	–	0.63	–	–	–	0.92

The splitting functions are MLG: this study; RR: Resovsky & Ritzwoller (1998); HT: He & Tromp (1996); Li: Li *et al.* (1991).

the elements of **A** is almost as large as that of **E** after rotation and ellipticity have been removed (0.41 μHz versus 0.44 μHz). We are currently investigating the consistency of the anelastic structure coefficients between modes.

We again compare the elastic splitting function with those of H&T and R&R. The three splitting functions agree rather well (Fig. 9b and Table 3), although the correlation between our map and the R&R map is fairly low. The reason for this is a moderate negative correlation of the degree 6 structure and a rather small correlation in degree 4. Also, the amplitude of degree 6 is very small in the H&T map and hence contributes little to the overall correlation with other maps. In fact, we rarely find good correlation with (and between) other maps at degree 6. The overall correlation between our map and the R&R map using only degrees 2 and 4 is much better (0.89).

As in the synthetic test, the splitting matrix for ${}_2S_4$ requires more events for a stable inversion than does ${}_1S_5$; our optimal choice is nine events. The elastic part of ${}_2S_4$ again agrees rather well with the splitting functions of H&T and R&R (see Fig. 9c and Table 3) but our map agrees better with the R&R map. Omitting degree 6 of the maps increases the correlation coefficient between our map and the R&R map to 0.90, which is comparable to that between the R&R and H&T maps. We have also experimented with the simultaneous inversion of the splitting matrices for ${}_1S_5$ and ${}_2S_4$. The resulting blocks corresponding to the splitting matrices of ${}_1S_5$ and ${}_2S_4$ are indeed comparable to those obtained from separate inversions. The non-diagonal cross-coupling blocks are significant in size, as has been found by Resovsky & Ritzwoller (1995, 1998), and can be used to constrain Earth structure of odd-harmonic degree.

Example 3: core-sensitive modes

We now consider two sets of core-sensitive modes, one of harmonic degree 1 and one of degree 2. The first set includes ${}_8S_1$ and ${}_{13}S_1$. The compressional energy densities for both of these modes have significant tails into the inner core but ${}_{13}S_1$ also has significant sensitivity to inner core shear velocity structure.

The inversions for the splitting matrices of both modes are very stable and only a few events are required. The combination of the Bolivian and the Kuril Islands events provides the basic structure of the splitting matrix of ${}_8S_1$ and changes are minor when more events are included. It is interesting to note that both the receiver strips and the splitting matrix do not change significantly with the inclusion or exclusion of the fundamental mode ${}_0S_{20}$ (which strongly overlaps with ${}_8S_1$ for standard 1-D models). We assume this is because the difference in harmonic degrees means that the process of computing receiver strips essentially rejects the contribution of ${}_0S_{20}$, although the fact that we are taking long records and are starting relatively late (Table 2) also suppresses the fundamental mode.

For ${}_{13}S_1$, the Bolivian event alone constrains the basic structure of **H**, although we take several events to improve the SNR. For the final splitting matrices, we take seven events for ${}_8S_1$ and six events for ${}_{13}S_1$. There are striking differences between the splitting matrices and the splitting functions of the two multiplets (Figs 10 and 11). The signal in the matrix for ${}_{13}S_1$ is much larger than in that of ${}_8S_1$. The predictions for the contribution of whole mantle models such as S16B30 (Masters *et al.* 1996) are very similar in size for both modes, suggesting that the source of the difference of the splitting function has to be located in the inner core.

Another very interesting feature is the large anelastic matrix of ${}_{13}S_1$, which is an extremely robust result of the inversion. Of all the modes we have analysed so far (many inner-core-sensitive modes and most of the low-ℓ modes of the first few overtone branches), ${}_{13}S_1$ has the largest signal from 3-D attenuation and could indicate large-scale lateral variations (or anisotropy) in Q structure in the inner core.

A comparison of our splitting functions with those of other authors shows a strong correlation of our ${}_8S_1$ map with the R&R and H&T maps (Fig. 12a and Table 3), while our ${}_{13}S_1$ map correlates less well with the H&T map (the correlation coefficient 0.63 is roughly at the 85 per cent confidence level) (Fig. 12b and Table 3). We speculate that ignoring 3-D attenuation has led to bias in the elastic splitting function.

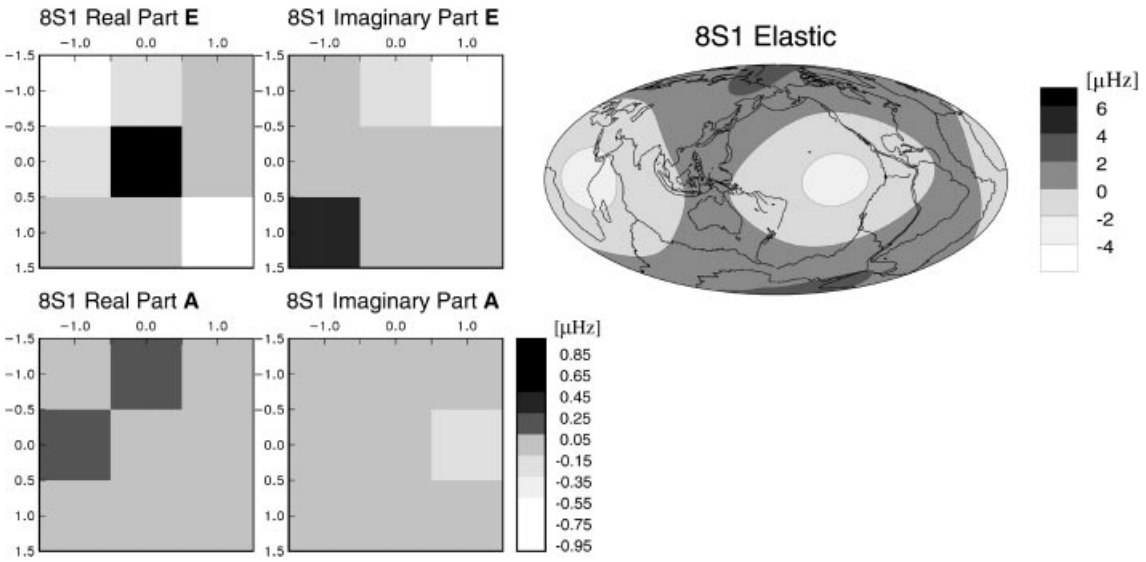

Figure 10. Splitting matrix and elastic splitting function for mode ${}_8S_1$, which has some sensitivity to structure in the inner core. Note that the signal is very small, especially for the anelastic part.

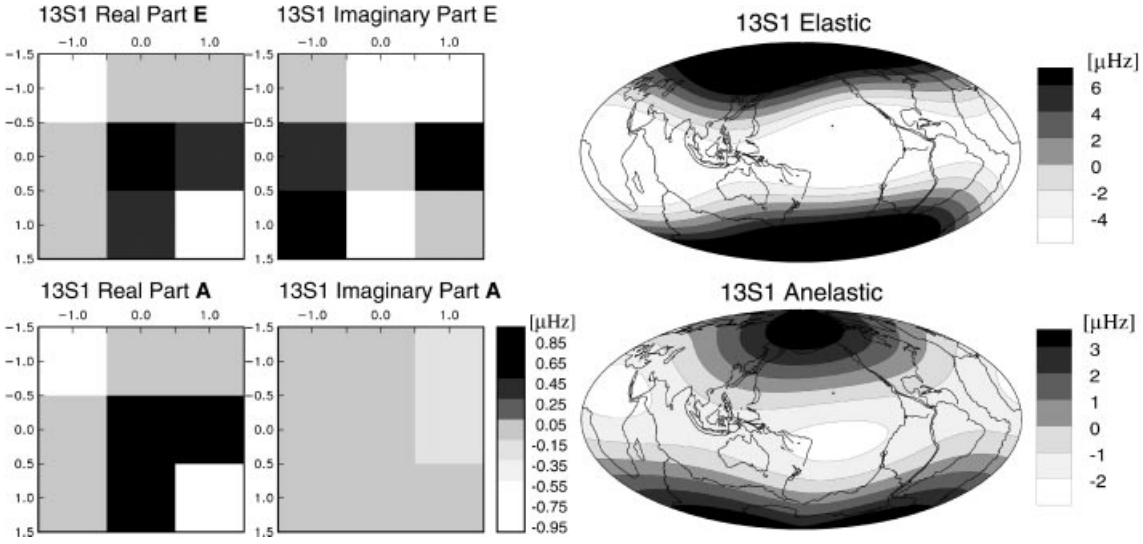

Figure 11. Splitting matrix and splitting functions for the anomalously split mode ${}_{13}S_1$. The anelastic splitting function is unusually large for this mode. Note that the elastic and anelastic parts are anticorrelated; that is, strong positive frequency shifts are associated with high attenuation.

Our last data example is the pair of modes ${}_{10}S_2$ and ${}_{13}S_2$. Both of these modes are sensitive to the inner core, although the energy densities of ${}_{10}S_2$ depend on the 1-D earth model chosen to calculate the eigenfunctions. Since both modes attenuate slowly, we start later in the record to suppress possible interference effects with neighbouring modes (Table 2).

For ${}_{13}S_2$ we find that taking three events constrains the basic structure of the splitting matrix, although we use seven events in the final estimate. Attempts using a combination of two events such as Bo and F or Bo and K (as done by H&T) fail in the sense that some of the m, $m' = \pm 2$ elements can be rather large. Our experience regarding the inversion for the splitting matrix of ${}_{10}S_2$ is rather similar to that of ${}_{13}S_2$. Taking three events is enough to constrain the basic structure of the splitting matrix, although we use seven events for the final estimate.

Since the anelastic part of the splitting matrix is small for both modes, we show elastic splitting functions only (Fig. 13). Also shown in Fig. 13 are the splitting functions of Li *et al.* (1991). The agreement between our and Li's splitting functions is excellent and the correlation coefficients are very high.

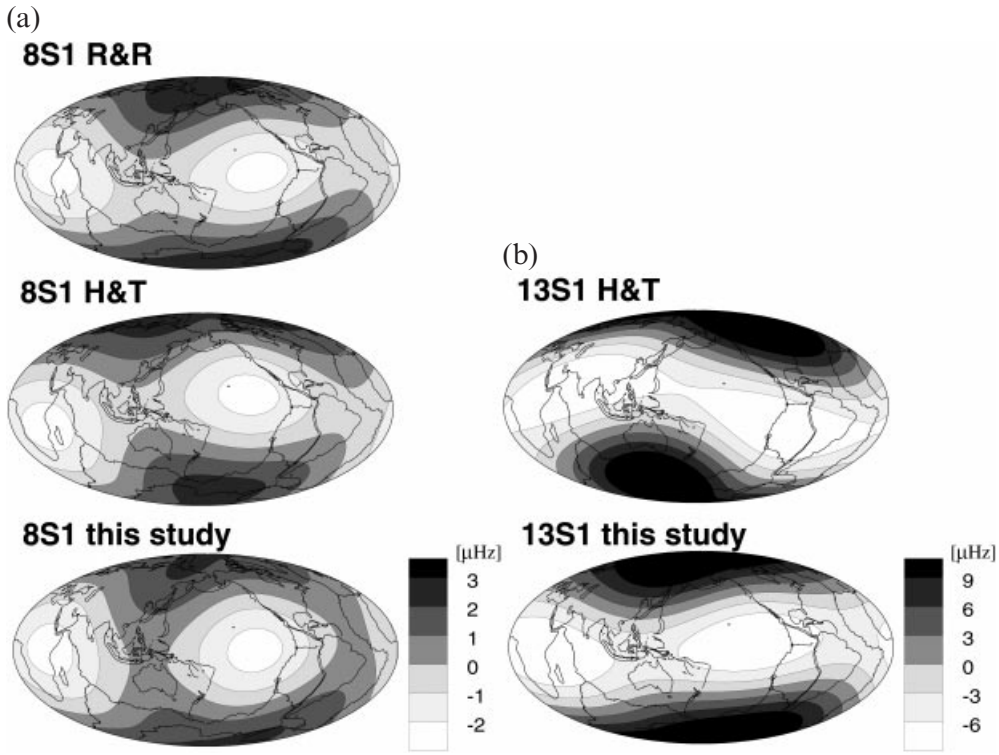

Figure 12. Elastic splitting functions for modes ${}_8S_1$ and ${}_{13}S_1$ compared with the splitting functions of R&R and H&T.

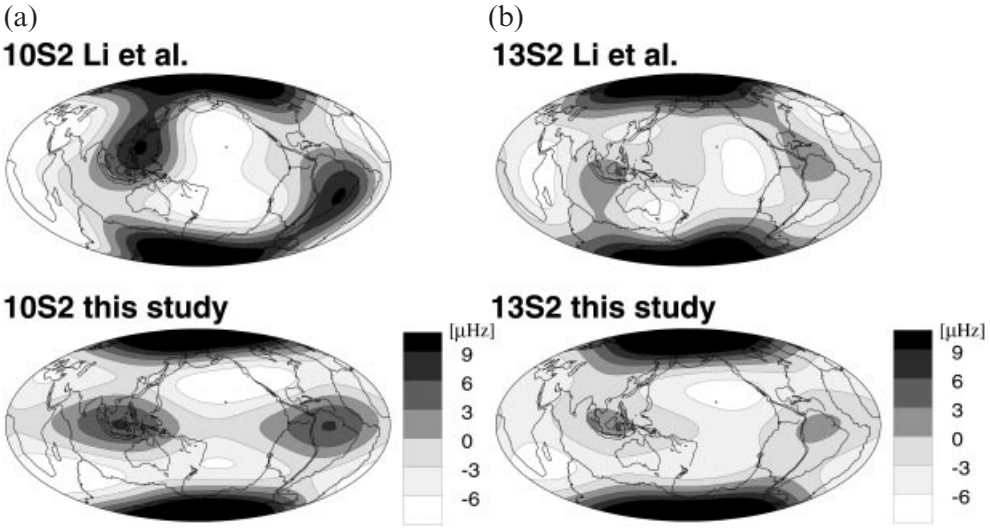

Figure 13. Elastic splitting functions for anomalously split modes ${}_{10}S_2$ and ${}_{13}S_2$ compared with the splitting functions of Li *et al.* (1991).

Furthermore, our splitting functions for ${}_{10}S_2$ and ${}_{13}S_2$ are remarkably highly correlated with each other—the correlation coefficient is 0.92. The splitting functions of both modes are dominated by the zonal structure coefficients c_2^0 and c_4^0. Much of the non-zonal contribution ($t \neq 0$) in the splitting functions is caused by structure in the mantle, although some residual structure from the inner core is detectable. The alignment of the non-zonal patterns in these splitting functions is better than 5°—this gives an idea of the geographic precision of the splitting functions and suggests that such data may be used to detect possible rotation of the inner core (as suggested by Sharrock & Woodhouse 1998). Indeed, the similarity of the splitting functions determined by Li *et al.* (1991) using events between 1977 and 1985 to our splitting functions (which use events from 1994 to 1998) suggests that relative inner core rotation is small.

DISCUSSION AND CONCLUSIONS

We have presented a matrix autoregressive (AR) method for estimating the splitting matrices of free-oscillation multiplets and have demonstrated its potential by applying it to records of some recent large earthquakes. The algorithm basically consists of two steps: the construction of receiver strips followed by reconstruction of the splitting matrix using the autoregressive property of the receiver strips. The splitting matrix can be uniquely decomposed into a part that governs elastic structure and a part that governs anelastic structure, both of which can be visualized by their splitting functions after inversion for elastic and anelastic structure coefficients.

The AR technique will generally be more efficient and robust than current methods (e.g. ISF) when the number of recordings of an event is larger than the total number of singlets being analysed. The insensitivity of the technique to source mechanism is a particular benefit since large earthquakes can often have complicated source mechanisms. This can become a significant problem for ISF when analysing high-frequency modes.

Our experiments indicate that the AR method works well when the number of nearly degenerate singlets within the multiplet is smaller than the number of events providing good recordings of the multiplet. In practical terms, with the current data set we must restrict attention to multiplets with harmonic degree less than about 10. Obviously, this restriction will become less severe as time progresses.

Our applications to real data show that the current generation of elastic splitting functions usually show reasonable agreement at degrees 2 and 4 (with some important exceptions), although disagreement at shorter wavelengths is common. The systematic application of the AR method to a large number of modes will allow us to assess this problem in the future. Also, we find some stable *anelastic* splitting functions for a few low harmonic degree modes, indicating large-scale strong lateral variations (or anisotropy) in attenuation in the inner core of the Earth. The detailed analysis of such modes will be presented in a later contribution.

Receiver strips and their AR properties can be used in other ways too. We have already shown that the construction of receiver strips allows the detection of timing errors and instrument response problems without any knowledge of the earthquake source. As another example, it is possible to interrogate the data from a large event using eq. (6) to ask whether a splitting matrix has changed over time—say due to rotation of the inner core. This removes the need to compare splitting functions derived from new and old data (as we have done in Fig. 13) and provides the most robust estimate of the relative rotation of the inner core (Laske & Masters 1999). Finally, we note that the point source approximation fails for many of the earthquakes we are dealing with, even at long periods. Inspection of eq. (5) shows that, once $\mathbf{P}$ has been determined, it is straightforward to estimate the source vector of a mode, $\mathbf{a}(0) = \mathbf{P}(\omega)^{-1} \cdot \mathbf{b}(\omega)$, although, for high SNR cases, the source vector can be estimated by integrating the receiver strips over the frequency band spanned by the multiplet (see Appendix A). The source vectors for many modes can then be interpreted in terms of a specific model of faulting or in terms of an expansion in spatial and temporal moment tensors. We expect this approach to be successful since the usual trade-off between the effects of source and structure on the seismogram has been removed.

ACKNOWLEDGMENTS

This research was made possible by the dedicated work of the personnel who run global seismic networks: Geoscope, IDA, IRIS, Mednet, Geofon, BFO and the USGS, and by the IRIS and Geoscope data centers, which greatly facilitate access to the data. We gratefully acknowledge support by grants EAR96-28494, EAR95-08113 and EAR97-06056 from the National Science Foundation. GM also wishes to thank Bob Parker and Cathy Constable for extensive discussions of this work. We thank Joe Resovsky for a helpful review of this manuscript.

REFERENCES

Dahlen, F.A., 1968. The normal modes of a rotating, elliptical earth, *Geophys. J. R. astr. Soc.,* **16,** 329–367.

Dahlen, F.A., 1982. The effect of data windows on the estimation of free oscillation parameters, *Geophys. J. R. astr. Soc.,* **69,** 537–549.

Dahlen, F.A. & Tromp, J., 1998. *Theoretical Global Seismology,* Princeton University Press, Princeton, NJ.

Eberlein, P.J., 1970. Solution to the complex eigenproblem by a norm reducing Jacobi type method, *Num. Math.,* **14,** 232–245.

Efron, B., 1982. The jackknife, the bootstrap and other resampling plans, *SIAM, Series in Applied Mathematics,* **38**.

Giardini, D., Li, X.-D. & Woodhouse, J.H., 1987. Three-dimensional structure of the earth from splitting in free oscillation spectra, *Nature,* **325,** 405–411.

Giardini, D., Li, X.-D. & Woodhouse, J.H., 1988. Splitting functions of long period normal modes of the earth, *J. geophys. Res.,* **93,** 13 716–13 742.

Gilbert, F., 1971. The diagonal sum rule and averaged eigenfrequencies, *Geophys. J. R. astr. Soc.,* **23,** 119–123.

Gilbert, F. & Dziewonski, A.M., 1975. An application of normal mode theory to the retrieval of structural parameters and source mechanisms from seismic spectra, *Phil. Trans. R. Soc. Lond.,* **A278,** 187–269.

Gilbert, F. & Woodhouse, J.H., 2000. Determination of structure coefficients from splitting matrices, *Geophys. J. Int.,* **141**.

Golub, G.H. & Reinsch, C., 1971. Singular value decompositions and least squares solutions, *Linear Algebra,* pp. 134–151, eds. Wilkinson, J.H. & Reinsch, C., Springer Verlag, New York.

Golub, G.H. & VanLoan, C.R., 1983. *Matrix Computations,* Johns Hopkins University Press, Baltimore, MD.

Harris, F., 1978. On the use of windows for harmonic analysis with the discrete Fourier transform, *Proc. IEEE,* **66,** 51–83.

He, X. & Tromp, J., 1996. Normal mode constraints on the structure of the Earth, *J. geophys. Res.,* **101,** 20 053–20 082.

Henson, I.H., 1989. Multiplet coupling of the normal modes of an elliptical, transversely isotropic, *Earth Geophys. J. Int.,* **98,** 457–459.

Jackson, D.D., 1972. Interpretation of inaccurate, insufficient and inconsistent data, *Geophys. J. R. astr. Soc.,* **28,** 97–109.

Landau, L.D. & Lifshitz, E.M., 1958. *Quantum Mechanics,* Addison Wesley, MA.

Laske, G. & Masters, G., 1999. Limits on differential rotation of the inner core from an analysis of Earth's free oscillations, *Nature,* **402,** 66–68.

Li, X.-D., Giardini, D. & Woodhouse, J.H., 1991. Large-scale, three-dimensional, even degree structure of the Earth from splitting of long-period normal modes, *J. geophys. Res.,* **96,** 551–577.

Lindberg, C.R. & Park, J., 1987. Multiple-taper spectral analysis of terrestrial free oscillations: Part II, *Geophys. J. R. astr. Soc.,* **91,** 795–836.

Masters, G., Johnson, S., Laske, G. & Bolton, H., 1996. A shear velocity model of the mantle, *Phil. Trans. R. Soc. Lond.,* **A354,** 1385–1411.

Park, J. & Gilbert, F., 1986. Coupled free oscillations of an aspherical dissipative rotating earth: Galerkin theory, *J. geophys. Res.,* **91,** 7241–7260.

Resovsky, J.S. & Ritzwoller, M.H., 1995. Constraining odd-degree mantle structure with normal modes, *Geophys. Res. Lett,* **22,** 2301–2304.

Resovsky, J.S. & Ritzwoller, M.H., 1998. New and refined constraints on three-dimensional Earth structure from normal modes below 3 mHz, *J. geophys. Res,* **103,** 783–810.

Ritzwoller, M., Masters, G. & Gilbert, F., 1986. Observations of anomalous splitting and their interpretation in terms of aspherical structure, *J. geophys. Res.,* **91,** 10 203–10 228.

Ritzwoller, M., Masters, G. & Gilbert, F., 1988. Constraining aspherical structure with low frequency interaction coefficients: application to uncoupled multiplets, *J. geophys. Res.,* **93,** 6369–6396.

Sharrock, D.S. & Woodhouse, J.H., 1998. Investigation of time dependent inner core structure by the analysis of free oscillation spectra, *Earth Planets Space,* **50,** 1013–1018.

Thomson, D.J., 1982. Spectrum estimation and harmonic analysis, *IEEE Proc.,* **70,** 1055–1096.

van Huffel, S., 1997. Recent advances in total least squares techniques and errors-in-variables modeling, *Proc 2nd Int. Workshop on TLS,* SIAM, Philadelphia.

van Huffel, S. & Vandewalle, J., 1991. The total least squares problem: computational aspects and analysis, *Frontiers in Applied Mathematics,* Vol. 9, SIAM, Philadelphia.

Widmer, R., Masters, G. & Gilbert, F., 1992. Observably split multiplets—data analysis and interpretation in terms of large-scale aspherical structure, *Geophys. J. Int.,* **111,** 559–576.

Wilkinson, J.H. & Reinsch, C., 1971. *Handbook for Automatic Computation,* Vol. 2, *Linear Algebra,* Springer-Verlag, New York.

Woodhouse, J.H., 1980. The coupling and attenuation of nearly resonant multiplets in the earth's free oscillation spectrum, *Geophys. J. R. astr. Soc.,* **61,** 261–283.

Woodhouse, J.H. & Dahlen, F.A., 1978. The effect of a general aspherical perturbation on the free oscillations of the earth, *Geophys. J. R. astr. Soc.,* **53,** 335–354.

Woodhouse, J.H. & Dziewonski, A.M., 1984. Mapping of the upper mantle: three-dimensional modeling of earth structure by inversion of seismic waveforms, *J. geophys. Res.,* **89,** 5953–5986.

Woodhouse, J.H. & Giardini, D., 1985. Inversion for the splitting function of isolated low order normal mode multiplets, *EOS, Trans. Am. geophys. Un.,* **66,** 300.

Woodhouse, J.H. & Girnius, T.P., 1982. Surface waves and free oscillations in a regionalized earth model, *Geophys. J. R. astr. Soc.,* **68,** 653–673.

Zürn, W. & Widmer, R., 1995. On noise reduction in vertical seismic records below 2 mHz using local barometric pressure, *Geophys. Res. Lett.,* **22,** 3537–3540.

APPENDIX A: ESTIMATION OF SOURCE VECTORS

Consider eq. (5) in the frequency domain:

$$\mathbf{b}(\omega) = \mathbf{P}(\omega) \cdot \mathbf{a}(0)\,,$$

where the eigenvalue decomposition of $\mathbf{P}(\omega)$ can be written

$$\mathbf{P}(\omega) = \mathbf{U} \cdot \mathbf{C}(\omega) \cdot \mathbf{U}^{-1}$$

and $\mathbf{C}(\omega)$ is a diagonal matrix of singlet resonance functions. Suppose we integrate across a frequency band, $\Delta\omega$, that spans

the multiplet

$$\boldsymbol{\beta} = \int_{\Delta\omega} \mathbf{b}(\omega)\, d\omega = \mathbf{U} \cdot \int_{\Delta\omega} \mathbf{C}(\omega)\, d\omega \cdot \mathbf{U}^{-1} \cdot \mathbf{a}(0)\,. \tag{A1}$$

Integrals of resonance functions are insensitive to the attenuation value or to the exact value of the singlet frequency (Gilbert & Dziewonski 1975), so we can write

$$\gamma \mathbf{I} = \int_{\Delta\omega} \mathbf{C}(\omega)\, d\omega\,,$$

where γ is a constant that can be computed. Substitution into eq. (A1) gives

$$\mathbf{a}(0) = \gamma^{-1} \boldsymbol{\beta}\,.$$

Thus, each element of the source vector is proportional to the integral of a receiver strip across the frequency band spanned by the multiplet. If more than one multiplet is present, this procedure returns the sum of the source vectors.